

Microstrip Patch versus Dielectric Resonator Antenna Bearing All Commonly Used Feeds

An experimental study to choose the right element.

Debatosh Guha and Chandrakanta Kumar

Microstrip patches and dielectric resonators (DRs) are two low-profile variants of modern microwave and wireless antennas. However, the DR antenna (DRA) is relatively new and still passing through the stages of development. Both variants are quite similar in terms of performance and characteristics. This article focuses on a meaningful comparative study where we have considered all commonly used feed mechanisms such as

coaxial probe, microstrip line, and rectangular aperture for both antennas operating near the same frequency. Circular geometry, i.e., cylindrical DRA (CDRA) and circular microstrip patch antenna (CMPA), have been chosen, and a systematic investigation based on thorough experiments has been executed. Multiple sets of prototypes have been fabricated and measured at 4 GHz. All available data have been furnished and compared, indicating relative advantages and disadvantages. This comparative study should provide qualitative and quantitative instructions to a designer for choosing the right element and corresponding feed based on design requirement and feasibility.

Digital Object Identifier 10.1109/MAP.2015.2501231
Date of publication: 17 February 2016

INTRODUCTION

The DRA started its journey in 1983 [1], [2] as an alternative to the microstrip patch; however, it still has not yet been fully explored in terms of applications at the industrial level. DRA technology suffers from several inherent limitations, which are primarily related to the physical properties of the material, their machining, and bonding with the application platform. In recent years, however, the antenna community has been greatly involved in DRA research. Newer features need to be explored to meet the needs of advanced miniaturized handheld and portable communication devices in all possible bands of communications.

Although proposed in 1953 [3], microstrips earned the attention of the antenna community between 1972 and 1974 [4], [5], i.e., about a decade before the inception of DRA, and by the 1980s, it had occupied almost every sector of wireless and microwave communications of our day-to-day life. Some of its inherent limitations, such as narrow operating bandwidth and high cross-polarized (XP) radiation, have been addressed [6]–[12] and resolved. But due to several known reasons, the DRA appears to be a possible replacement for the microstrip patch, especially at higher frequencies.

Indeed, both antenna types are very close in some aspects as they both have similar feed mechanisms and radiation patterns. Although they have their individual merit and potential, very few works so far have addressed comparative study between the DRA and the microstrip patch antenna (MPA) [13]–[15].

In [13], the performances of 8×8 arrays of aperture-coupled microstrip patches and DRAs were compared at 25 GHz with both the arrays being fed by microstrip corporate feeds. The DRA array shows wider bandwidth and higher gain. Another contemporary work reported a comparison based on the measured results obtained at 10 GHz using probe-fed configurations [14]. This comparison was biased toward DRA, since for the ease of comparison, an identical $\epsilon_r(10.2)$ was chosen for the DRA as well as the microstrip substrate. Such a high value of $\epsilon_r(10.2)$ as a substrate would naturally cause a very narrow impedance bandwidth and a low gain. In reality, MPA designers would prefer $\epsilon_r < 3$.

Another recent work [15] has compared a CDRA with a CMPA at 35 GHz, which also seems to be biased toward the DRA, since the choice of operating frequency is not suitable for a microstrip patch radiator. Unlike [14], the DRA and MPA have been designed using two different dielectrics with relative permittivities $\epsilon_{rd} = 10$ and $\epsilon_{rs} = 2.2$, respectively. But, it would be important to note that [15] considered only a microstrip line as the feed.

Neither of these studies can give a complete and comprehensive idea about the relative performance when they are fed by different feeding techniques and both are designed to operate at a common realistic domain of frequency.

Microstrip patches and dielectric resonators are two low-profile variants of modern microwave and wireless antennas.

The present investigation is aimed at alleviating these lacunas and generating practical information to help the practicing engineers and designers. In addition, this would help both the microstrip and DRA researchers in identifying the most appropriate antenna element for a particular use. The choice is not straightforward and depends on a variety of specifica-

tions and requirements.

For our study, we have considered all commonly used feeding techniques including coaxial-feed, planar microstrip feed, and electromagnetically coupled aperture feed for a set of CMPAs and CDRA resonating at their respective fundamental mode around 4 GHz. The test frequency has been chosen based on the operating frequency that is acceptable for both antennas and the physical dimension of the elements along with their machining, fabrication, and measurements, which should be feasible in a laboratory setup.

This will provide a pure comparative study based on the experimental data obtained with multiple units of the prototypes. Their optimized designs have been obtained using simulated results [16]. For realizing a circular microstrip patch resonating at 4 GHz, we have used a commercial PTFE substrate. Its DRA version operating at the same frequency has been realized in the form of a CDRA. The detailed design aspects, including the realization of the prototypes, have been discussed, measured results have been documented, and relative merits and demerits of each antenna have been identified for each type of feed mechanism. The results shed light on the selection of the appropriate antenna element with the correct feed, which varies from case to case and application to application.

RADIATING MODE AND DESIGN OF INDIVIDUAL RADIATING ELEMENT

One of the important aspects of antenna design is to select the proper operating mode, which, in turn, determines the radiation pattern. Both the CMPA and the CDRA can be operated in multiple modes at multiple frequencies, which may result in different radiation patterns such as broadside peak, broadside null, and multiple lobes. These modes and corresponding radiation patterns can be found in [6], [7], and [17]–[21] for MPAs and in [22]–[28] for DRAs.

For our investigation, broadside radiation with a single main lobe has been considered for both antennas, and, as such, they need to be operated in their fundamental mode, i.e., TM_{11} for a CMPA and $HEM_{11\delta}$ for a CDRA.

Figure 1 depicts the electric current and field distributions due to a CMPA. The metallic surfaces at the top and the bottom form a cavity surrounded by a magnetic wall, which resonates at [29]

$$f_{r,11} = \frac{\alpha_{11}c}{2\pi r_{m,\text{eff}} \sqrt{\epsilon_{rs,\text{eff}}}}, \quad (1)$$

where $\alpha_{11} = 1.8412$ is the first zero of the derivative of the Bessel function of order one, c is the velocity of light in free space, $r_{m,eff}$ is the effective patch radius, and $\epsilon_{rs,eff}$ is the effective relative permittivity of the substrate [29].

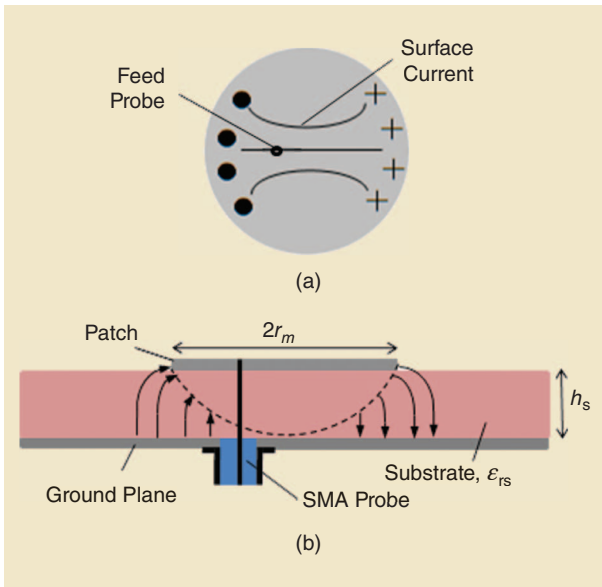


FIGURE 1. The field distribution inside the CMPA in dominant TM_{11} mode: (a) the currents and fields on the patch (top view) and (b) the side view of the antenna.

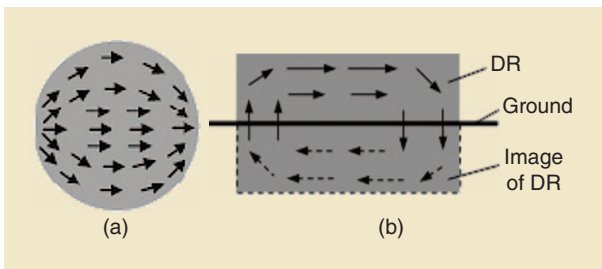


FIGURE 2. The field distribution inside the CDRA in dominant $HEM_{11\delta}$ mode. (a) Top view. (b) Side view.

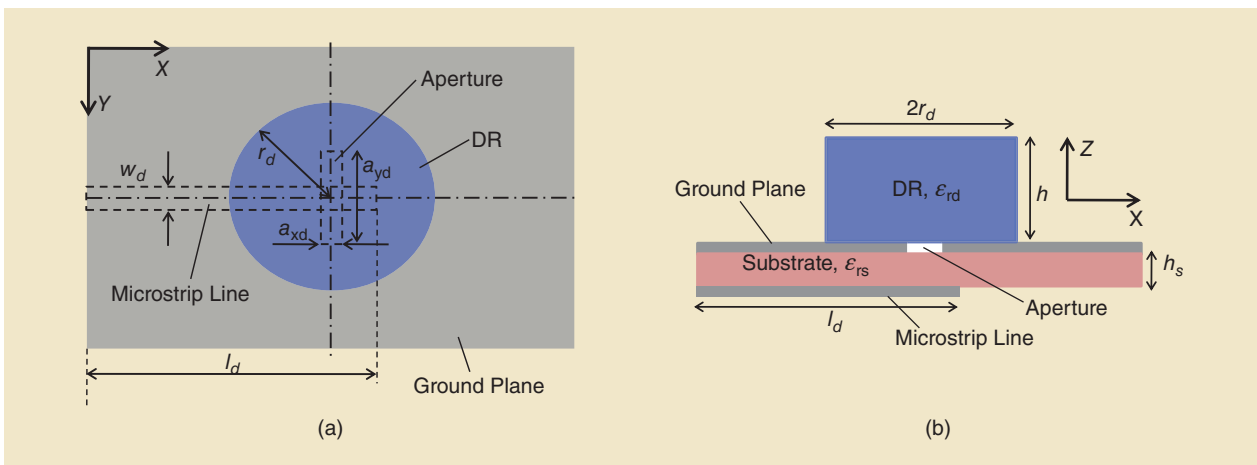


FIGURE 3. The configuration of an aperture-fed CDRA. (a) Top view. (b) Side view.

Figure 2 shows the electric fields due to $HEM_{11\delta}$ resonating mode in a CDRA. A DRA, mounted on a metallic ground plane, creates an electric image, resulting in an increase in effective height, which is just double the physical height. Its resonant frequency is then determined as [22]

$$f_r = \frac{c}{2\pi r_d \sqrt{\epsilon_{rd}}} \left[1.71 + \frac{r_d}{h} + 0.1578 \left(\frac{r_d}{h} \right)^2 \right], \quad (2)$$

where r_d and h represent its radius and height, respectively, and ϵ_{rd} the relative permittivity of the material. For the study, the chosen operating frequency of each antenna element is 4 GHz. Since each CMPA has been etched from a RT 5870 substrate with $\epsilon_{rs} = 2.33$ and $h_s = 1.575$ mm, using (1) its radius has been determined to be about 14 mm. Similarly, (2) results in $r_d = h = 10$ mm for the given material with $\epsilon_{rd} = 10$.

DIFFERENT FEEDS, PROTOTYPES, AND FABRICATION

Three different types of feeds—coaxial probe, microstrip line, and aperture coupling—are common for both CMPA and CDRA, specifically, to excite them with their respective fundamental mode. However, the choice of the feed depends on the deployment of the antenna and its associated circuitry. For example, the coaxial probe appears to be the proper choice for the antenna that is separated from its transmit/receive unit. If the antenna element shares the same circuit board as an integrated unit, a microstrip-line-fed or aperture-coupled configuration appears to be convenient. It is important to note that primary antenna characteristics such as bandwidth, gain, and polarization purity change considerably with the feed network.

The microstrip prototypes have been etched from the RT5870 substrate with $\epsilon_{rs} = 2.33$ and $h_s = 1.575$ mm. Each CDRA unit has been shaped from the Eccostock HiK rod with $\epsilon_{rd} = 10$. Microstrip line feeding is very common, and this has been realized using the same substrate with a single layer. The aperture-coupled configuration for a DRA, as well as for a CMPA, is bit different from that used in microstrip feed and they are schematically shown in Figures 3 and 4, respectively. Such an aperture feed has also been realized using the same RT5870 substrate. Radiall's R125.464.270W 50- Ω SMA

connector with a central pin of 1.3-mm diameter has been used for coaxial feeding in both microstrips and DRAs.

Printed feeds and antennas have been coprocessed using a single substrate to avoid any variation caused by substrate parameters and the fabrication process. The photographs of the prototypes bearing three different feeds are shown in Figures 5 and 6. The values of the parameters have been indicated in Figures 5 and 6, respectively.

While both types of antennas are low profile and integratable, the microstrip patch is easily printable. On the other hand, the DRA requires precision machining, as well as additional efforts to affix it on the ground plane or feeding circuit. A machinable DRA material, which was a challenge even a few years ago, is now commercially available. But antenna engineers would prefer softer and lighter layer materials for practical applications. The inevitable thin layer of air between

The present investigation is aimed at alleviating these lacunas and generating practical information to help the practicing engineers and designers.

the DRA and the metallic ground plane always affects the antenna performance.

Considering the prior physical constraints, the MPA scores heavily over the DRA. Moreover, the MPA is conformable over a curved surface, which is not feasible for DRAs.

DOMINANT MODE RESONANCE AND OPERATING BANDWIDTH

Agilent's E8363B vector network analyzer, calibrated using the N4692-60001 electronic calibration kit, has been used to measure the reflection coefficients of the antennas. The measured results are presented in Figures 7 and 8 and summarized in Table 1. For each feed configuration, optimum S_{11} responses of the CMPA and the CDRA have been compared using measured and simulated data in Figure 7. The measured data closely corroborate the simulated predictions. They reveal that the DRA always has a wider impedance bandwidth.

A comparison on the basis of the feed configurations is studied in Figure 8. All the feeds show comparable data for MPA, but this not true for DRAs. The impedance matching is found to be a major issue in DRA specifically, and its possible reasons are attributed to an unavoidable air gap between the dielectric and ground plane, dielectric, and probe pin, misalignment of DRA with respect to the aperture, or a relative misalignment between the aperture and feeding strip. Any of these or some of their combinations are found to occur in most of the practical cases. Therefore, matching bandwidth ($S_{11} < -10$ dB) becomes too sensitive to the type of feed. As discussed, the aperture feed appears to be very sensitive (Table 1). As per the measured data furnished in Table 1, the circular patch operates over about 2–3% bandwidth, whereas that of a DRA varies over approximately 6–10%. A coaxial probe feed offers the best impedance matching for both the antennas.

Therefore, matching bandwidth ($S_{11} < -10$ dB) becomes too sensitive to the type of feed. As discussed, the aperture feed appears to be very sensitive (Table 1). As per the measured data furnished in Table 1, the circular patch operates over about 2–3% bandwidth, whereas that of a DRA varies over approximately 6–10%. A coaxial probe feed offers the best impedance matching for both the antennas.

RADIATION CHARACTERISTICS

The radiation properties of the prototypes have been measured in an anechoic chamber with an automated measurement setup using a MI-1797 receiver and MI-3000 data acquisition software. A pyramidal horn with a very low cross-polarization level is used as the transmitting antenna, and the antennas under test (AUT), mounted on the positioner, are used as the receiving antenna. The

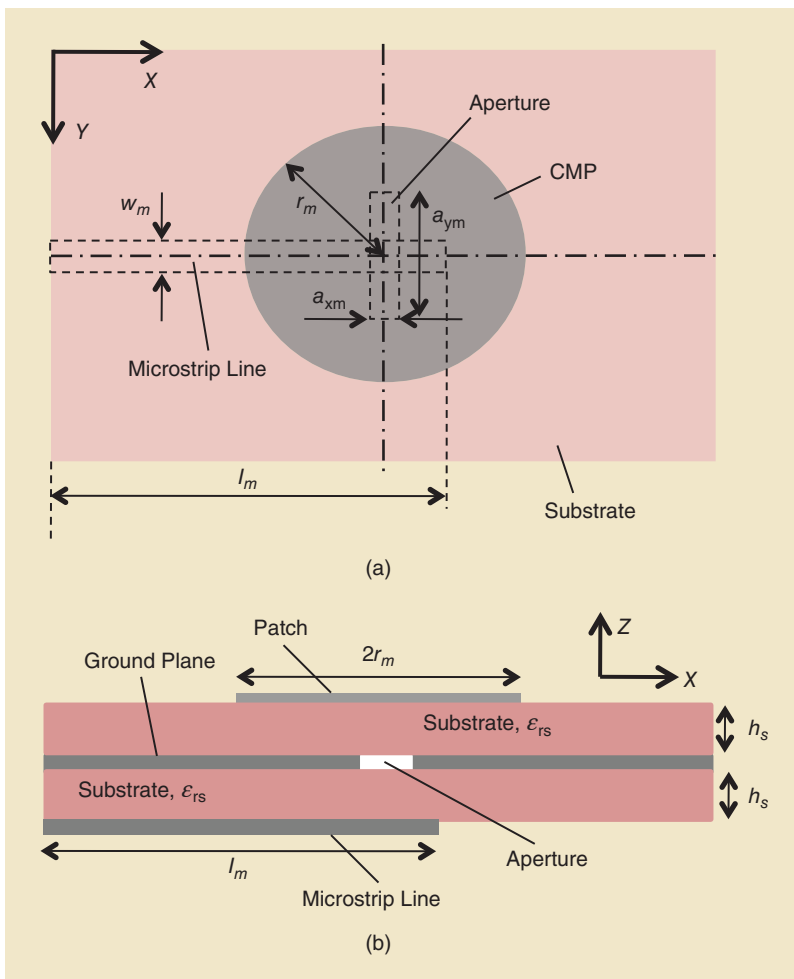


FIGURE 4. The configuration of an aperture-fed CMPA. (a) Top view. (b) Side view.

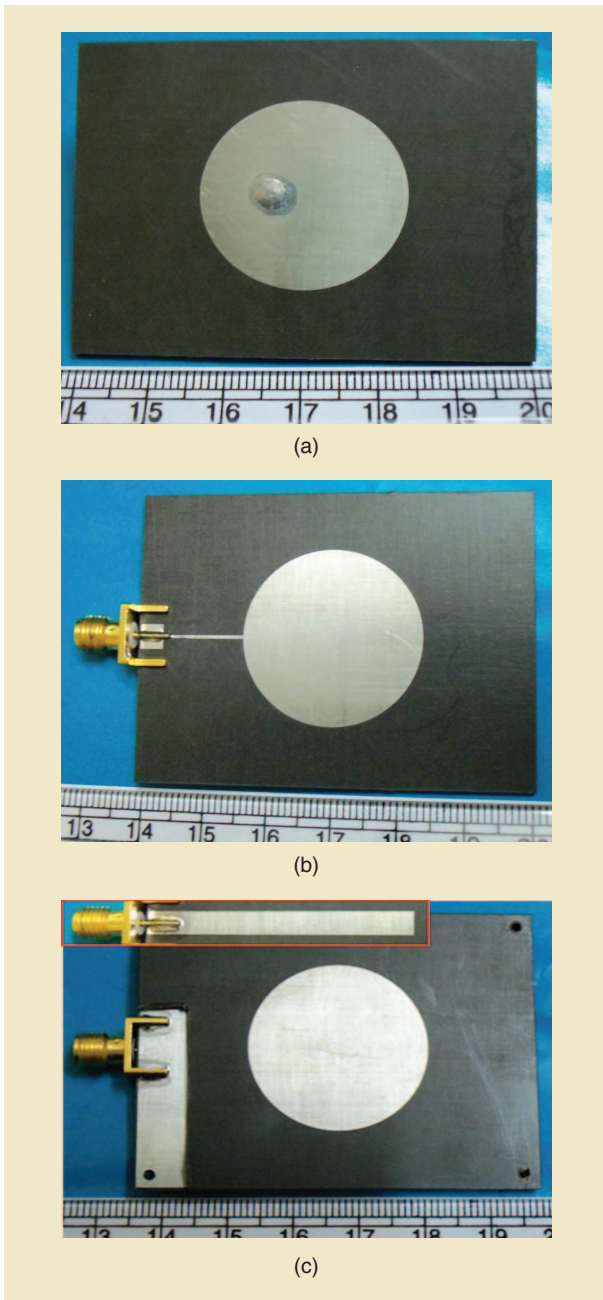


FIGURE 5. The photographs of the CMPAs with different feeds. The parameters are $r_m = 13.7$ mm, substrate: $\epsilon_{rs} = 2.33$, $h_s = 1.575$ mm, and ground plane 60 mm \times 45 mm. (a) A probe-fed patch with a probe diameter of $d = 1.3$ mm and a probe location of $\rho = 3.7$ mm. (b) A microstrip-line line-fed patch: narrower line 0.53 mm \times 12.8 mm and wider line 3.33 mm (width) \times 3.6 mm. (c) An aperture-fed patch. Inset—the feed line behind the ground plane. $a_{xm} = 2$ mm, $a_{ym} = 10$ mm, $w_m = 4.2$ mm, and $l_m = 36.6$ mm.

roll axis of the AUT positioner is adjusted for perfect copolar and cross-polar alignment with the transmitting horn. The gain of the antennas is measured using the standard gain horn using the method of substitution. The measured data along with the corresponding simulated results are discussed in the following sections.

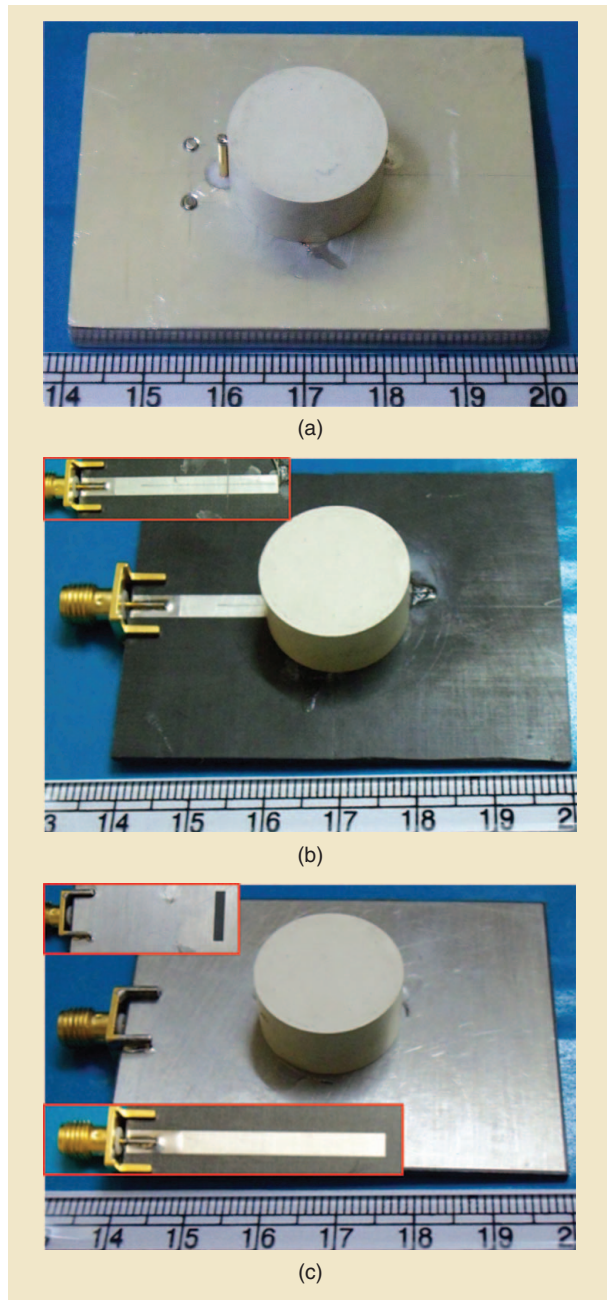


FIGURE 6. The photographs of the CDRA with different feeds. The parameters are DR: $\epsilon_{rd} = 10$, $r_d = 10$ mm, and $h = 10$ mm; PTFE substrate: $\epsilon_{rs} = 2.33$, $h_s = 1.575$ mm, and ground plane 60 mm \times 45 mm. (a) A probe-fed DRA with a probe diameter of $d = 1.3$ mm and a probe length of 8.4 mm. (b) The microstrip-line-fed DRA: inset—feed is 3.5 mm \times 39.3 mm. (c) An aperture-fed DRA: inset—the feed line behind the ground plane and the aperture. $a_{xd} = 2$ mm, $a_{yd} = 10$ mm, $w_d = 3.5$ mm, and $l_d = 39.4$ mm.

COPOLARIZED PATTERNS AND GAIN

The measured and simulated radiation characteristics using different feed configurations for both the antennas are shown and compared in Figures 9–12. The measurements are found to corroborate the simulated predictions. The radiation patterns appear symmetric in the H-plane for all

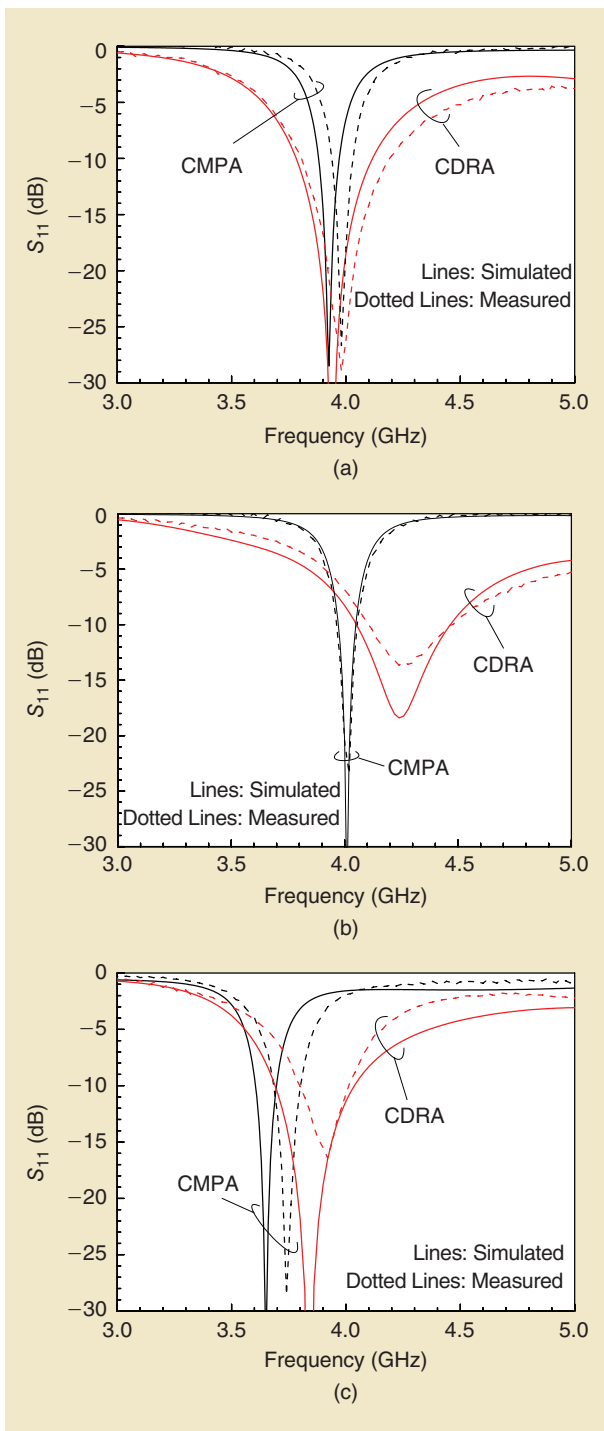


FIGURE 7. The measured and simulated plots of reflection coefficient versus frequency for the CDRA and CMPAs with different feed configurations. (a) Probe fed. (b) Microstrip line fed. (c) Aperture fed. The parameters are the same as in Figures 5 and 6.

the configurations. However, some degree of asymmetry is observed in the E-plane, which is revealed consistently in all the feed configurations for both the antennas.

The measured radiation data, obtained through a series of experiments, are shown in Table 2, and the available simulated

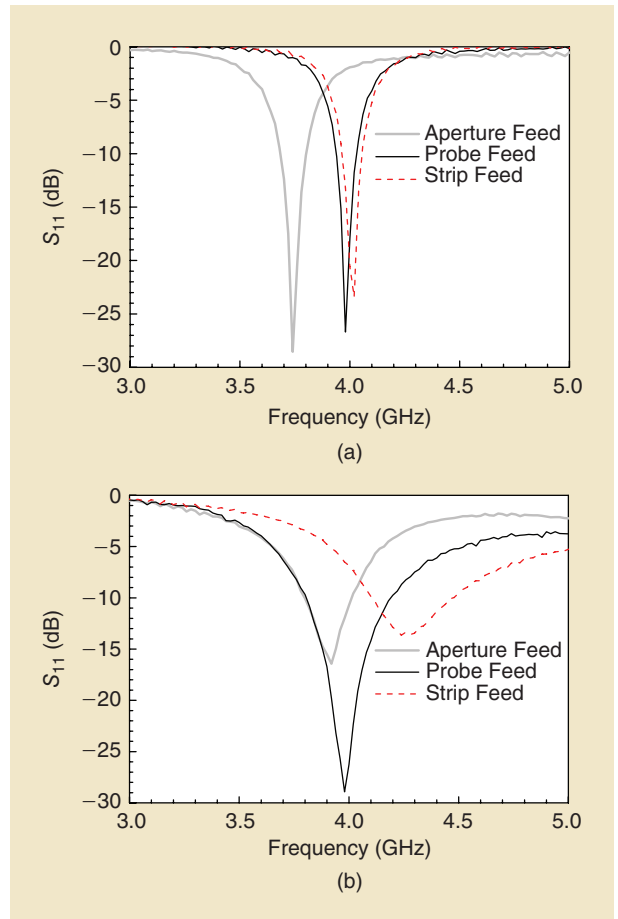


FIGURE 8. The measured S_{11} plots of the antennas with different feed configurations: (a) CMPA and (b) CDRA.

values are included within parentheses for ready information and comparison. They indicate several important observations:

- A CDRA offers either comparable or wider beamwidth compared with a CMPA, although one particular measurement for microstrip-fed CDRA for the E-plane pattern shows considerable deviation from the predicted value. This may be attributed to some degree to the unwanted radiation from the exposed part of the microstrip feed line, resulting in asymmetry in E-plane radiation and hence the unexpectedly narrow beamwidth ($\sim 69^\circ$).
- The peak gain of a CDRA (with $\epsilon_r = 10$) is always lower than that of a CMPA and it is found to be about 0.8-1.1 dB down.
- A DRA has an efficiency greater than the CMPA with a typical difference of about 10%.

CROSS-POLARIZED RADIATIONS

XP radiation is the measure of the unwanted polarization of the radiated fields. In a linearly polarized antenna, it indicates those radiated fields that are orthogonal to the primary plane of polarization. The XP is an unavoidable phenomenon in practical antennas and is therefore very important to estimate before applying to a practical application. This is examined in Figures 9–12. The XP radiation is supposed to be undetectable in the E-plane, which is corroborated by the measured

data obtained with all three feeds. But in the H-plane, the XP grows in an oblique direction from a very low value at boresight. A comparative study of H-plane XP values is presented in Figure 12. The aperture-fed configurations of CDRA and CMPA

exhibit considerably lower XP, which is expected due to the symmetry in the feed. Of the other two, the probe appears to be a better choice for CMPA, but for a CDRA, the microstrip feed appears to be better.

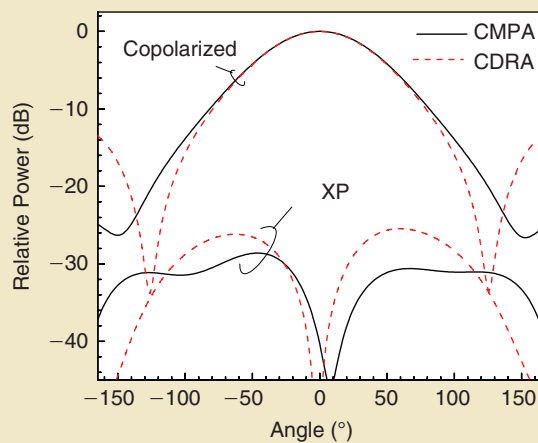
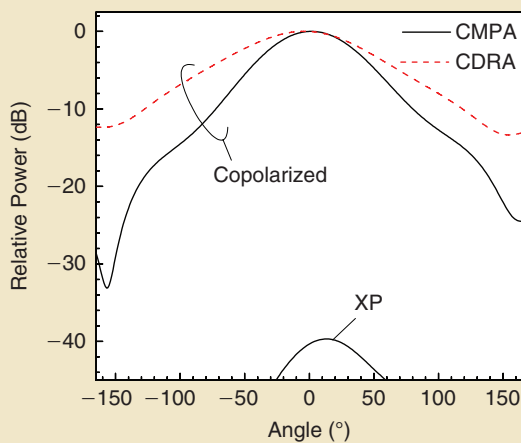
The key point from the discussion on the copolarized and XP radiation patterns is that the DRAs and MPAs have similar radiation patterns with a particular feed. However, with respect to the pattern symmetry and XP performance, the aperture feed is a better choice, even though it is relatively complex.

RADIATION EFFICIENCY

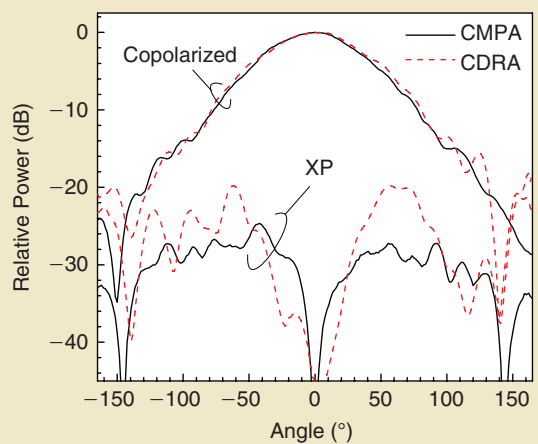
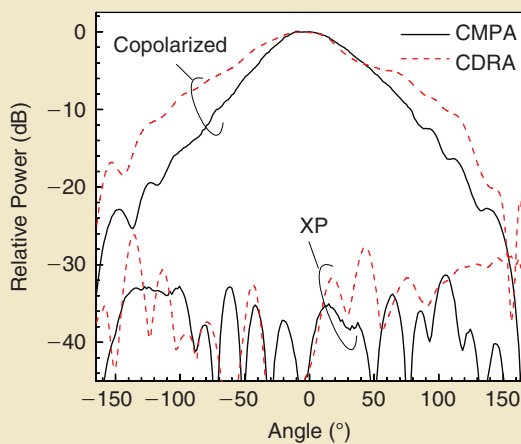
Radiation efficiency measures the percentage of the total input power that is actually radiated. The rest of the power is returned or dissipated as mismatch, conduction, or dielectric losses. We have measured the efficiency of each of the prototypes, using the Wheeler cap method [30], [31]. The input resistances R_{in} of

TABLE 1. THE COMPARISON OF BANDWIDTH CHARACTERISTICS BASED ON THE MEASURED AND SIMULATED DATA PARAMETERS AS IN FIGURES 5 AND 6.

| Bandwidth ($S_{11} < -10$ dB) | | CMPAs | | | CDRAs | | |
|-----------------------------------|------------------|-------|--------|----------|-------|--------|----------|
| | | Probe | MSLine | Aperture | Probe | MSLine | Aperture |
| Absolute (MHz) | Simulated values | 90 | 80 | 100 | 330 | 415 | 355 |
| | Measured values | 90 | 90 | 110 | 380 | 350 | 210 |
| Percent (%) | Simulated values | 2.2 | 2.0 | 2.5 | 8.3 | 9.7 | 9.2 |
| | Measured values | 2.2 | 2.2 | 2.9 | 9.5 | 8.3 | 5.4 |



(a)



(b)

E-Plane

H-Plane

FIGURE 9. Probe-fed configuration: measured and simulated radiation patterns at the respective center frequencies of CMPA and CDRA. (a) Simulated. (b) Measured. The parameters are the same as in Figures 5 and 6.

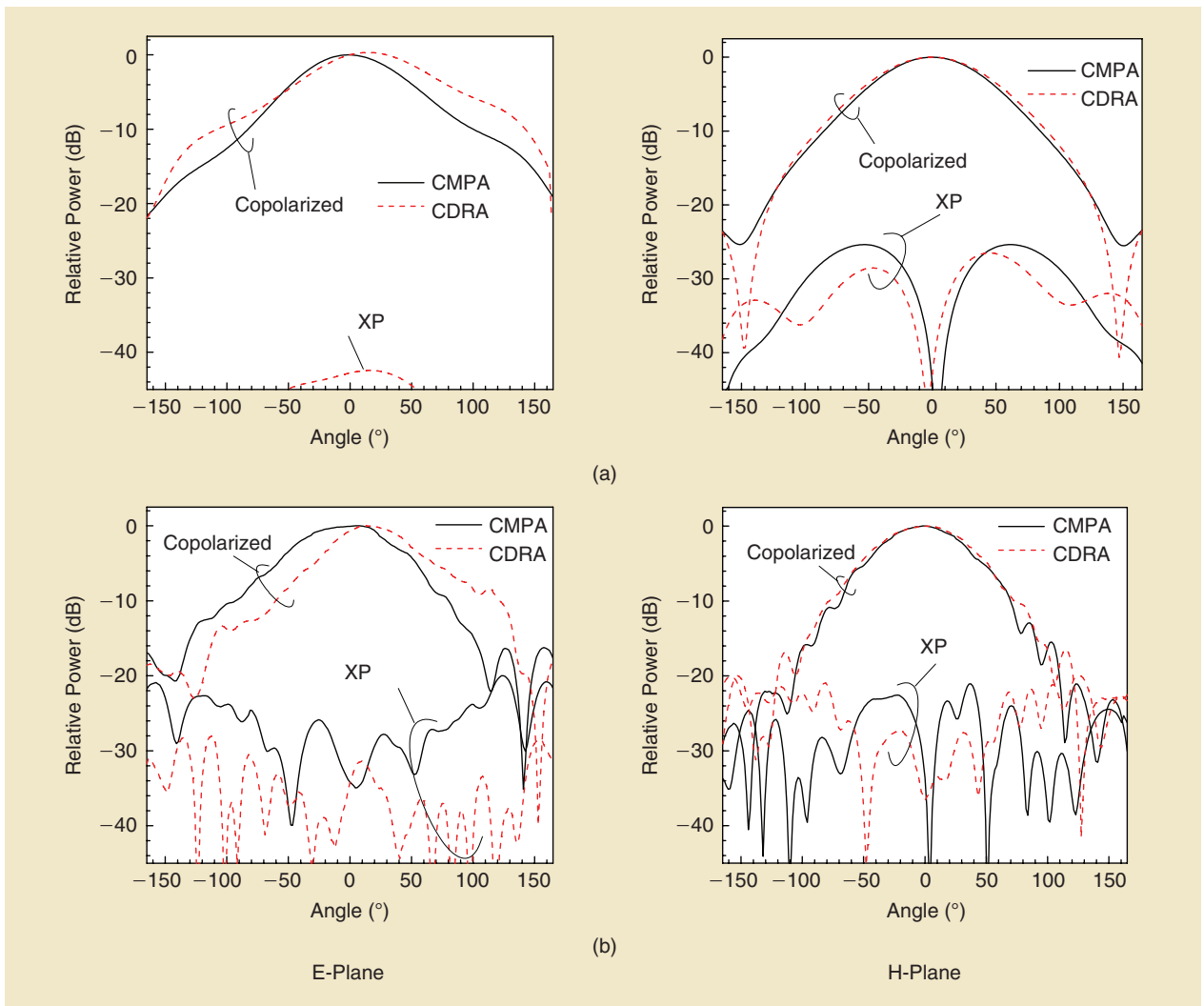


FIGURE 10. The microstrip line feed. (a) The measured and (b) the simulated radiation patterns at the respective center frequencies of CMPA and CDRA. The parameters are the same as in Figures 5 and 6.

the antennas with and without the Wheeler cap are measured using the network analyzer. The input resistance without the cap $R_{in-nc} = R_{rad} + R_{loss}$, where R_{rad} is the radiation resistance and R_{loss} is the total loss resistance. The resistance with the Wheeler cap is $R_{in-cap} = R_{loss}$. The efficiency η (in %) of the antenna is then given by

$$\eta = \frac{R_{in-nc} - R_{in-cap}}{R_{in-nc}} \times 100. \quad (3)$$

The result obtained using (3) for each antenna has been provided in Table 2. The measurements show that the DRA efficiency is always about 10% higher than that of the microstrip for any set of feed networks. It is interesting that the probe-fed configurations earn the highest efficiency score with a DRA of 96% and microstrip of 87%. In the other two planar feeds,

loss in the microstrip lines is responsible for degrading the efficiency and show comparable numerical values.

DRA PERFORMANCE AS A FUNCTION OF MATERIAL PERMITTIVITY

Although a very high relative permittivity is not recommended for DRA, an antenna engineer may be curious to know about the order of magnitude of the change in DRA characteristics if the relative permittivity is varied over a large range of values. To address this issue, a set of representative results has been generated [16]; these results are all acquired while the antenna dimensions unaltered. The results are furnished in Table 3 and some significant observations are as follows:

- The matching bandwidth and the antenna gain are significantly enhanced with lowered permittivity, due to reductions in the Q value of the DRA.

A pyramidal horn with a very low cross-polarization level is used as the feed.

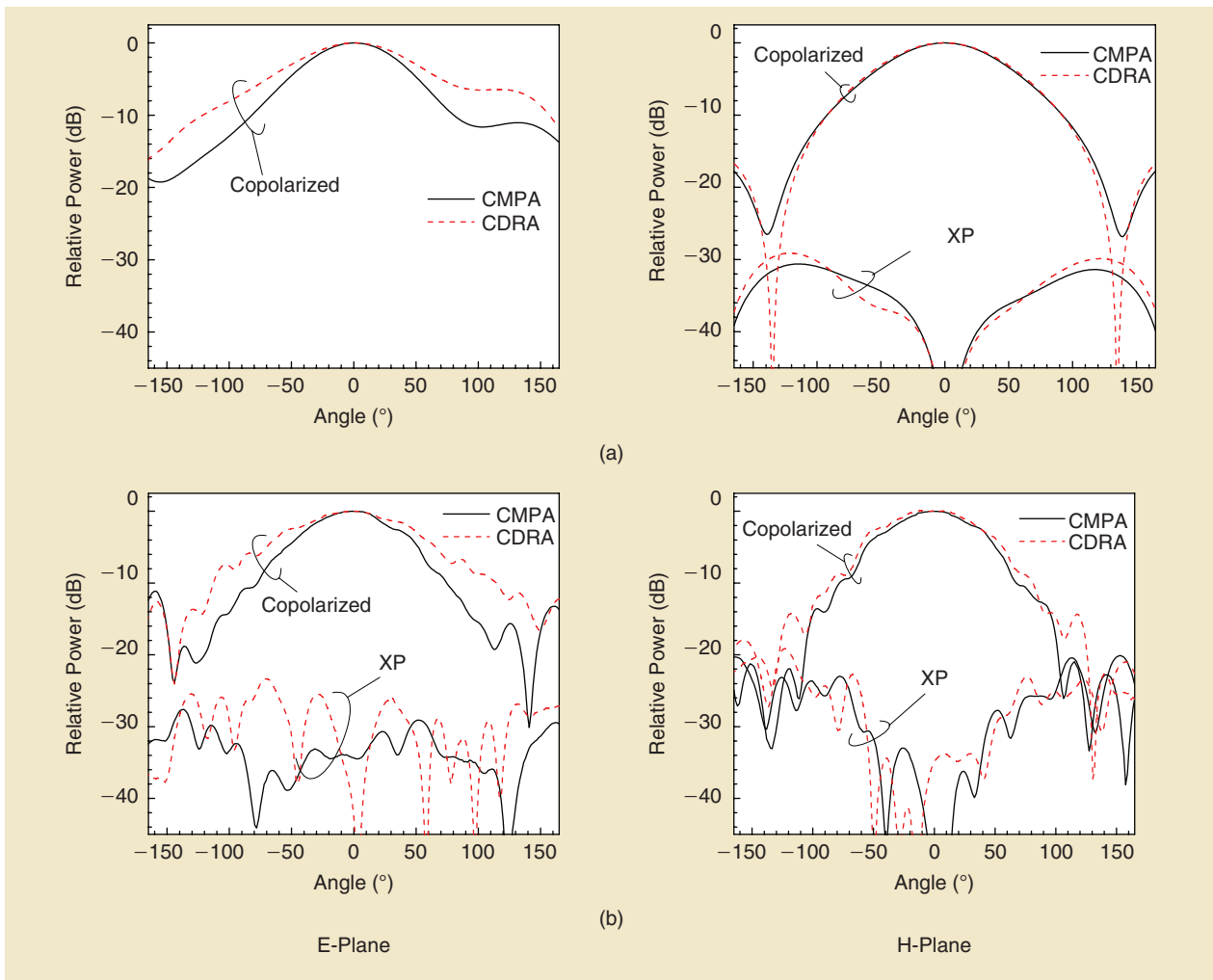


FIGURE 11. The aperture feed. (a) The measured and (b) the simulated radiation patterns at the respective center frequencies of CMPA and CDRA. The parameters are the same as in Figures 5 and 6.

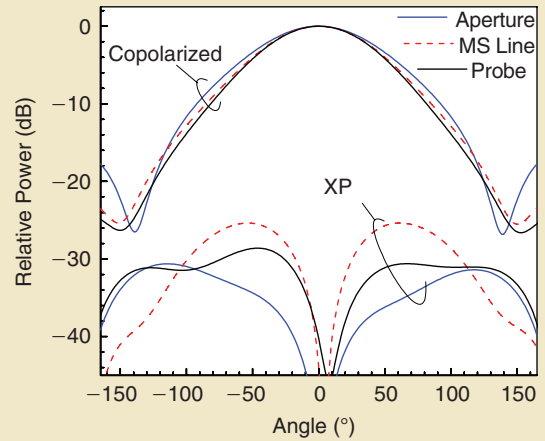
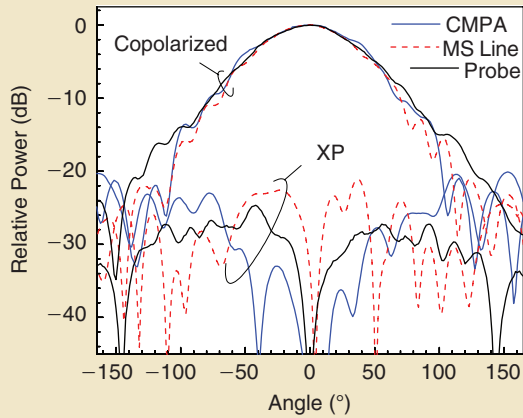
- Low ϵ_{rd} (≈ 6) suffers from an excitation issue because of low Q ; this effect is more prominent in microstrip-feed configurations.
- For each ϵ_{rd} , the effect of the feed configuration is clearly visible in determining the antenna characteristics. The probe and the aperture feeds are comparable in terms of the bandwidth and gain to the microstrip feed because it marginally improved, especially for $\epsilon_{rd} \geq 10$.

CONCLUSIONS AND RECOMMENDATION

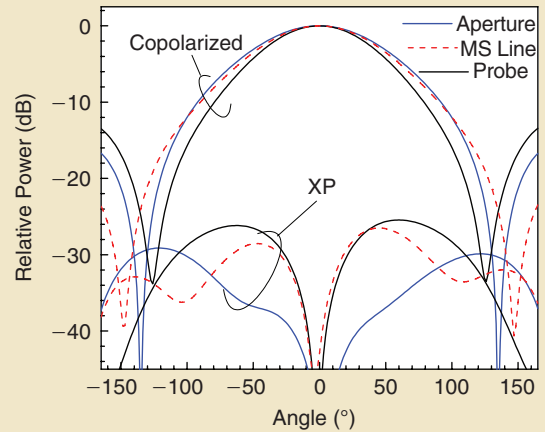
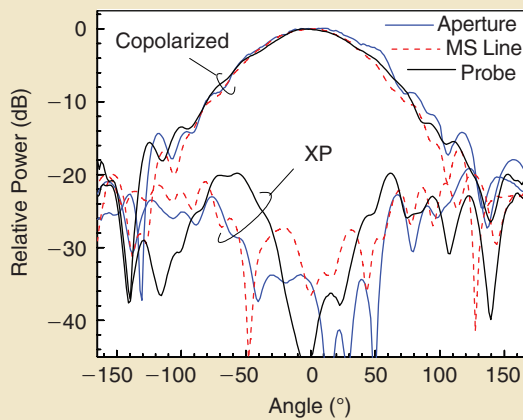
The results obtained with two sets of antennas having different types of feed mechanisms give some practical insights into choosing or recommending proper radiating element, either microstrip or DR, depending on the practical requirement and the design specification. This may be summarized as follows:

Printed feeds and antennas have been coprocessed using a single substrate to avoid any variation caused by substrate parameters and the fabrication process.

- The DRA is well ahead of the MPA in terms of wider bandwidth and higher efficiency but at the cost of compromising with the gain value by approximately 1 dB. It would be relevant to note that the characteristics of both types of antennas are dependent on their respective dielectric properties.
- Integrated DRAs or MPAs require microstrip-line or aperture feeds, which are superior in terms of XP performance. However, if efficiency is the concern, the coaxial probe feed is preferred.
- Although the DRA seems to outperform the MPA in some ways, mechanical processing and stability of the MPA are advantages when compared to the DRA.



Microstrip Patch Antenna



Dielectric Resonator Antenna

(a)

(b)

FIGURE 12. The H-plane radiation (a) measured and (b) simulated patterns at the respective center frequencies of the antennas with different types of feeds. The parameters are the same as in Figures 5 and 6.

TABLE 2. THE COMPARISON OF PRIMARY ANTENNA RADIATION CHARACTERISTICS.

| Radiation Parameters | | Probe | | MSLine | | Aperture | |
|----------------------|---------|--------------|--------------|--------------|--------------|--------------|--------------|
| | | MPA | DRA | MPA | DRA | MPA | DRA |
| Beamwidth (deg) | E-plane | 69 (73) | 78 (110) | 87 (90) | 69 (110) | 82.5 (78) | 110 (99) |
| | H-plane | 80 (70) | 80 (70) | 75 (89) | 81 (90) | 84 (88) | 99 (90) |
| Gain (dBi) | | 6.5 (6.6) | 5.4 (5.4) | 6.1 (6.4) | 5.2 (5.6) | 5.8 (5.9) | 4.8 (5.1) |
| Efficiency (%) | | 87 | 96 | 80 | 92 | 82 | 93 |

The values within parenthesis are simulated predictions parameters as in Figures 5 and 6.

TABLE 3. THE CDRA PERFORMANCE FOR VARYING MATERIAL PERMITTIVITY.

| Feed Type | Antenna Characteristics | ϵ_{rd} | | |
|-----------------|-------------------------|-----------------|------|-------|
| | | 20 | 10 | 6 |
| Probe | Reso. freq.(GHz) | 2.88 | 3.95 | 4.95 |
| | Bandwidth (%) | 3.48 | 8.3 | 12.82 |
| | Gain (dBi) | 3.72 | 5.3 | 5.64 |
| Aperture | Reso. freq. (GHz) | 2.71 | 3.86 | 4.93 |
| | Bandwidth (%) | 3.21 | 9.2 | 12.64 |
| | Gain (dBi) | 3.70 | 5.1 | 5.64 |
| Microstrip Line | Reso. freq. (GHz) | 3.04 | 4.25 | * |
| | Bandwidth (%) | 4.91 | 9.7 | — |
| | Gain (dBi) | 4.08 | 5.66 | — |

* Difficult to excite due to poor impedance matching.
a = h = 10 mm and other parameters are the same as in Table 1, each DRA being optimally matched.

ACKNOWLEDGMENTS

We would like to thank D. Kundu and A.S. Guin for their help in this work during the initial phase and P. Gupta and C. Sarkar during the revision of this article. We would also like to thank the reviewers for their useful comments and suggestions.

AUTHOR INFORMATION

Debatosh Guha (dguha@ieee.org) is a professor at the Institute of Radio Physics and Electronics, the University of Calcutta, India, and is currently the HAL chair professor in the Electronics and Electrical Communication Engineering Department, the Indian Institute of Technology Kharagpur, India. He is a fellow of the Indian National Academy of Engineering and National Academy of Sciences, India, and an associate editor of *IEEE Antennas and Wireless Propagation Letters*. He has received international awards including the Raj Mittra Travel Grant Award for Senior Researcher 2012, URSI Young Scientist Award 1996, and Jawaharlal Nehru Memorial Fund Prize 1984. He is a member of the review board of *IEEE Transactions on Antennas and Propagation*; *IEEE Transactions on Microwave Theory and Techniques*; *IEEE Antennas and Propagation Magazine*; *IET Microwaves, Antennas, and Propagation*; and *IET Electronics Letters*. His current research interests include defected ground structure for antenna application, unresolved issues of microstrip antenna design, ultrawideband hybrid antennas, unconventional radiating modes and new feed concepts for dielectric resonator antennas, and compact high-gain antennas for wireless equipment.

Chandrakanta Kumar (kumarchk@ieee.org) received his M.Tech. and Ph.D. degrees in radio physics and electronics from the University of Calcutta, India. He is currently an engineer at ISRO Satellite Centre, Bangalore. He is actively involved in the design of antenna systems for the Indian space program and related ground stations. He served as an antenna systems project manager for the first Indian mission to the moon, Chandrayaan-1, GSAT-12, and ASTROSAT spacecrafts. As a deputy project director, he is responsible for the RF systems of the Chandrayaan-2 mission. He has published approximately 70 publications in international journals and conferences. He is a recipient of the 2011 Prof. S.N. Mitra Memorial Award from IETE, India, the 2009 Young Scientist Award, and the 2008 Team Excellence Award of the Indian Space Research Organisation. He is a fellow of IETE, India, a Senior Member of the IEEE, and life member of the Astronautical Society of India. He also serves on the board of reviewers for many international journals.

REFERENCES

- [1] M. W. McAllister, and S. A. Long, "Rectangular dielectric resonator antenna," *IEEE Electron. Lett.*, vol. 19, no. 6, pp. 218–219, Mar., 1983.
- [2] S. A. Long, M. W. McAllister, and L. C. Shen, "The resonant cylindrical cavity antenna," *IEEE Trans. Antennas Propag.*, vol. 31, pp. 406–412, May 1983.
- [3] G. A. Deschamps, "Microstrip microwave antennas," presented at the 3rd USAF Symp. on Antennas, 1953.
- [4] J. Q. Howell, "Microstrip antennas," in *Dig. IEEE Int. Symp. Antennas Propagation*, Dec. 1972, pp. 177–180.
- [5] R. E. Munson, "Conformal microstrip antennas and microstrip phased arrays," *IEEE Trans. Antennas Propag.*, vol. 22, no. 1, pp. 74–78, 1974.
- [6] R. Garg, P. Bhartia, I. Bahl, and A. Ittipiboon, *Microstrip Antenna Design Handbook*. Norwood, MA: Artech House, 2001.

- [7] D. Guha and Y. M. M. Antar, Ed., *Microstrip and Printed Antennas New Trends, Techniques and Applications*. Hoboken, NJ: Wiley, 2010.
- [8] D. M. Pozar, "Microstrip antennas," *Proc. IEEE*, vol. 80, no. 1, pp. 79–91, Jan. 1992.
- [9] A. Petosa, A. Ittipiboon, and N. Gagnon, "Suppression of unwanted probe radiation in wideband probe-fed microstrip patches," *Electron. Lett.*, vol. 35, no. 5, pp. 355–357, Mar. 4, 1999.
- [10] K. L. Wong, C. L. Tang, and J. Y. Chiou, "Broad-band probe-fed patch antenna with a W-shaped ground plane," *IEEE Trans. Antennas Propag.*, vol. 50, no. 6, pp. 827–831, June 2002.
- [11] Z. N. Chen, and M. Y. W. Chia, "Broad-band suspended probe-fed plate antenna with low cross-polarization level," *IEEE Trans. Antennas Propag.*, vol. 51, no. 2, pp. 345–346, Feb. 2003.
- [12] C. Kumar and D. Guha, "Nature of cross-polarized radiations from probe-fed circular microstrip antennas and their suppression using different geometries of defected ground structure (DGS)," *IEEE Trans. Antennas Propag.*, vol. 60, no. 1, pp. 92–101, Jan. 2012.
- [13] A. Petosa, S. Thirakoune, M. Zuliani, and A. Ittipiboon, "Comparison between planar arrays of perforated DRAs and microstrip patches," *IEEE Antennas Propag. Soc. Int. Symp.*, 2005, vol. 2A, pp. 168–175.
- [14] R. Chair, A. A. Kishk, K. F. Lee, and D. Kajfez, "Performance comparisons between dielectric resonator antennas and printed microstrip patch antennas at X-band," *Microwave J.*, vol. 49, pp. 90–104, Jan. 31, 2006.
- [15] Q. Lai, G. Almpanis, C. Fumeaux, H. Benedickter, and R. Vahldieck, "Comparison of the radiation efficiency for the dielectric resonator antenna and the microstrip antenna at Ka band," *IEEE Trans. Antennas Propag.*, vol. 56, no. 11, pp. 3589–3592, Nov. 2008.
- [16] High frequency structure simulator (HFSS), Ansoft, v 11.1.
- [17] S. Biswas, D. Guha, and C. Kumar, "Control of higher harmonics and their radiations in microstrip antennas using compact defected ground structures," *IEEE Trans. Antennas Propag.*, vol. 61, no. 6, pp. 3349–3353, June 2013.
- [18] L. H. Chang, W. C. Lai, J. C. Cheng, and C. W. Hsue, "A symmetrical reconfigurable multipolarization circular patch antenna," *IEEE Antennas Wireless Propagat. Lett.*, vol. 13, pp. 87–90, Jan. 2014.
- [19] L. Cui, W. Wu, and D.-G. Fang, "Wideband circular patch antenna for pattern diversity application," *IEEE Antennas Wireless Propagat. Lett.*, vol. 14, pp. 1298–1301, Feb. 2015.
- [20] B. Babakhani, and S. Sharma, "Wideband frequency tunable concentric circular microstrip patch antenna with simultaneous polarization reconfiguration," *IEEE Antennas Propagat. Mag.*, vol. 57, no. 2, pp. 203–216, 2015.
- [21] J. Tak, S. Lee, and J. Choi, "All-textile higher order mode circular patch antenna for on-body to on-body communications," *IET Microwaves, Antennas Propag.*, vol. 9, no. 6, pp. 576–584, 2015.
- [22] A. Petosa, *Dielectric Resonator Antenna Handbook*. Norwood, MA: Artech House, 2007.
- [23] D. Guha, A. Banarjee, C. Kumar, and Y. M. M. Antar, "Higher order mode excitation for high gain broadside radiation from cylindrical dielectric resonator antennas," *IEEE Trans. Antennas Propag.*, vol. 60, no. 1, pp. 71–77, Jan. 2012.
- [24] A. Motevasselian, A. Ellgardt, and B. L. G. Jonsson, "A circularly polarized cylindrical dielectric resonator antenna using a helical exciter," *IEEE Trans. Antennas Propag.*, vol. 61, no. 3, pp. 1439–1443, Mar. 2013.
- [25] Y. X. Sun and K. W. Leung, "Dual-band and wideband dual-polarized cylindrical dielectric resonator antennas," *IEEE Antennas Wireless Propagat. Lett.*, vol. 12, pp. 384–387, Mar. 2013.
- [26] X. S. Fang, K. W. Leung, and K. M. Luk, "Theory and experiment of three-port polarization-diversity cylindrical dielectric resonator antenna," *IEEE Trans. Antennas Propag.*, vol. 62, no. 10, pp. 4945–4951, Oct. 2014.
- [27] Y. M. Pan, S. Y. Zheng, and B. J. Hu, "Design of dual-band omnidirectional cylindrical dielectric resonator antenna," *IEEE Antennas Wireless Propagat. Lett.*, vol. 13, pp. 710–713, Apr. 2014.
- [28] O. G. Avadanei, M. G. Banciu, and L. Nedelcu, "Higher-order modes in high-permittivity cylindrical dielectric resonator antenna excited by an off-centered rectangular slot," *IEEE Antennas Wireless Propagat. Lett.*, vol. 13, pp. 1585–1588, Aug. 2014.
- [29] D. Guha, "Resonant frequency of circular microstrip antennas with and without airgaps," *IEEE Trans. Antennas Propag.*, vol. 49, no. 1, pp. 55–59, Jan. 2001.
- [30] H. A. Wheeler, "The radianosphere around a small antenna," *Proc. IRE*, vol. 47, no. 8, pp. 1325–1331, 1959.
- [31] E. H. Newman, P. Bohley, and C. H. Walter, "Two methods for the measurement of antenna efficiency," *IEEE Trans. Antennas Propag.*, vol. 23, no. 4, pp. 457–461, July 1975.

